Molecular Transfer Characteristics of Air Between 40 and 140 GHz

HANS J. LIEBE, SENIOR MEMBER, IEEE

Abstract—**Radio wave propagation in the 40–140-GHz band through the first hundred kilometers of the clear atmosphere is strongly influenced by many (>30) lines of the oxygen microwave spectrum (O_2–MS) and to a lesser extent by water vapor. A unified treatment of molecular attenuation and phase dispersion is formulated whereby results of molecular physics are translated into frequency-, temperature-, and pressure-dependencies. The propagation factors are developed for O_2 continuum—($h < 10$ km) and line—($h > 20$ km) spectra taking into account pressure-broadening ($h < 40$ km), Zeeman-splitting ($h > 40$ km), and Doppler broadening ($h > 60$ km). The influence of water vapor is discussed briefly. The filter characteristics of dry air are evaluated for various path models. Examples of computer plots of attenuation and dispersion rates are given as a function of altitude h for homogeneous, zenith, and tangential path geometries through the 1962 U. S. standard atmosphere.**

I. INTRODUCTION

THE relatively stable dry air mass represents a unique filter over the 40–140-GHz range with transfer, shielding, and emission properties caused by the microwave spectrum of oxygen, and not found at any lower frequency. Atmospheric transmission data suitable to promote further exploitation of this largely unused portion of the extremely high frequency (EHF) spectrum have to be related to meteorological conditions as accurately as possible. Applications are dependent on the ability to describe the somewhat complicated interaction between microwaves and the molecules that comprise the atmosphere. Normally, concepts of molecular spectroscopy are not too familiar to radio engineers. This paper interprets theories that relate spectroscopic properties of the atmosphere to their molecular origin. The resulting calculation schemes are meant to derive transfer characteristics from meteorological parameters in most direct form. The reliability of such schemes is discussed in light of the existing body of experimental data. More recent analytical and theoretical studies of the oxygen microwave spectrum (O_2–MS) are considered which on several accounts are supported by on-going experimental work [1]–[4]. Many details and most of the references to the original work are left to a comprehensive report on the same topic [1].

The multiline structure of the O_2–MS around 60 GHz requires computer analysis since at ground level pressures more or less all lines contribute to one transmission value. Many workers evaluated atmospheric O_2–MS absorption [5], [6], [9], [12], [20]–[23], [26], [27]; we extend these calculations by including the effects of phase dispersion and by considering more recent laboratory work [2].

Signal analysis for propagation over atmospheric paths is facilitated in treating the medium as a linear system and applying the transfer function concept [5]. A transfer function is defined by

$$\tau = \exp\{-[(\alpha/20 \log e) + j(\phi_0 + \Delta\phi)]L\} \quad (1)$$

($20 \log e = 8.686$) for free propagation of radiation of frequency ν over the distance L. The solution of (1) for the clear atmosphere over the range $\nu \sim 40$–140 GHz requires consideration of the microwave spectra of the molecules O_2 and H_2O. The propagation factors (power attenuation α, phase delay ϕ_0, and phase dispersion $\Delta\phi$) are expressed in the form

$$\begin{aligned} \alpha &= 0.1820\nu(N_d'' + N_w'') \text{ dB/km} \\ \phi_0 &= 0.02095\nu N_0 \text{ rad/km} \\ \Delta\phi &= 0.029095\nu(\Delta N_d + \Delta N_w) \text{ rad/km} \end{aligned} \quad (2)^1$$

where for dry air

$$N_d'' = \sum_i [S/\gamma(1 + z^2)]_i \text{ ppm} \quad (3)$$

$$\Delta N_d = \sum_i [Sz/\gamma(1 + z^2)]_i \text{ ppm} \quad (4)$$

describes the O_2–MS extinction and dispersion as a sum of i Lorentzian lines. Water vapor is treated separately in Section II-D. The notation means: ν is the microwave frequency in gigahertz; S_i are the line strengths in hertz; γ_i are the linewidths in megahertz; $z_i = (\nu_{0^i} - \nu)/\gamma_i$ are dimensionless frequencies normalized for each line to multiples of γ; ν_{0^i} are the O_2–MS line center frequencies, i is a label for 44 lines of the O_2–MS, N_0 is the frequency-independent refractivity in parts per million, and N_w'' and ΔN_w are molecular extinction and dispersion spectra, respectively, due to water vapor, both in parts per million. Except for some possible modifications of the widths γ_i (Section II-C), we expect (3) and (4) to be valid for the pressure-broadened O_2–MS ($p \sim 1$–800 torr). In the following, the spectroscopic parameters are developed in terms of dry air and water vapor pressure, p and p_w in torr,[2] and temperature T in degrees Kelvin as

Manuscript received February 20, 1974; revised October 23, 1974 This work was supported in part by the NOAA-National Environmental Satellite Service under Order NA-755-73 and the U. S. Army Research Office (ARO 14-74).

The author is with the Institute for Telecommunication Sciences, Office of Telecommunications, the U. S. Department of Commerce, Boulder, Colo. 80302.

[1] $(4\pi/c)\ 10 \log e = 0.1820$ / $(2\pi/c) = 0.02095$ } when ν in gigahertz and N or ΔN in parts per million.

[2] The unit torr does not comply with recommended S.I. units. The conversion is 1 torr = 133.322 pascal (N/m^2).

they occur over altitudes, $h = 0 \approx 80$ km. The second part applies the U. S. Standard Atmosphere [7] $\{p(h)$ and $T(h)\}$ and numerical methods to predict transfer characteristics for various path geometries.

II. SPECTROSCOPIC PARAMETERS OF AIR

A. *Frequency-Independent Refractivity*

The nondispersive refraction of air is commonly expressed in parts per million by N-units[3]

$$N_0 = [pR^0 + p_w R_w{}^0(T)]/T. \quad (5)$$

The refractivity values for dry air and water vapor are $R^0 = 103.5$ and $R_w{}^0 = (95.5 + 499\ 500/T)$ ppm K/torr, respectively. These values have been measured at 48 and 61 GHz [8], [2].

B. *The O_2 Microwave Spectrum*

A complete theory of O_2–MS absorption was first given by Van Vleck [9], laboratory absorption measurements were reported by Artman and Gordon [10], and the refraction spectrum was treated by Zhevakin and Naumov [11]. More recently, it was the work leading to radiometric remote sensing of atmospheric temperature structure based on O_2–MS emission that expanded and refined the theory [12]–[14], [23], [28].

For all atmospheric transmission problems, it is sufficient to consider $i \leq 44$ individual lines. A molecular resonance implies that O_2 selectively absorbs (attenuation) and stores (phase dispersion), and randomly reradiates (incoherent noise) microwave energy. The salient line parameters—center frequency ν_0, strength S^0, and width γ^0—are listed in Table I either by the label i or by the rotational quantum number N. The line strengths S_i in (3) and (4) are given by [4]

$$S_i = 0.2090(\nu/\nu_0{}^i)p[S^0\psi(T)]_i \text{ Hz}. \quad (6)$$

The strength parameters $S_i{}^0$ are calculated at 300 K and the associated temperature dependences are

$$\psi(T)_i = (300/T)^3 \cdot \exp\{-6.895 \cdot 10^{-3} N(N+1)[(300/T) - 1]\}. \quad (7)$$

Each N-pair of lines possesses its own temperature dependence (Table I). At low temperatures ($\lesssim 250$ K) many of the lines with high N-numbers may be neglected.

The O_2–MS is greatly complicated by Zeeman splitting of each line into many components under the influence of the earth's magnitic field strength H. The Zeeman effect produces anisotropic, polarization-dependent transfers characteristics above $h \approx 40$ km. At these altitudes the lines are less than a few megahertz wide. We later discuss an example, but refer to [13], [28], and [1] for the involved calculations of frequency shift and line strength for the many Zeeman components of an O_2–MS line.

[3] Pressure proportionality is indicated in general for all appropriate parameters by a superscript ^{0}.

TABLE I
SPECTROSCOPIC PARAMETERS OF THE O_2 MICROWAVE LINE SPECTRUM (D-DOUBLET)

i	ν_0 [1] GHz		N + *)	N − *)	S° [1], [2] Hz/torr (300° K)	γ° (Eq. 8a) MHz/torr	
1	48.942 4			43	.000 024	1.41	
	49.451 4			41	.000 073	1.41	
	49.961 8			39	.000 216	1.41	
	50.473 6			37	.000 598	1.41	
5	50.987 3			35	.001 56	1.41	
	51.503 02			33	.003 86	1.41	
	52.021 17			31	.008 99	1.41	
	52.542 23			29	.019 71	1.41	
	53.066 80			27	.040 72	1.41	
10	53.595 68			25	.079 19	1.41	
	54.129 96			23	.144 8	1.45	
	54.671 145 (20)			21	.248 9	1.50	
	55.221 372 (20)			19	.401 2	1.54	
	55.783 819 (20)			17	.605 6	1.59	
15	56.264 778 (10)	D	1		.348 7	1.96	
	56.363 393 (20)			15	.853 9	1.64	
	56.968 180 (20)			13	1.120	1.68	
	57.612 49			11	1.360	1.73	
	58.323 885 (10)			9	1.515 0	1.77	
20	58.446 580 (10)	D	3		.925 (30)	1.91	
	59.164 215 (10)			7	1.526	1.82	
	59.590 978 (10)		5		1.341	1.87	
	60.306 044 (10)			5	1.349	1.87	
	60.434 776 (10)	D	7		1.563(30)	1.82(3)	
25	61.150 565 (5)		9		1.590(20)	1.77(2)	
	61.800 169 (10)		11		1.459	1.73	
	62.411 223 (10)		13		1.227	1.68	
	62.486 255 (10)	D		3	.9634	1.91	
	62.998 00		15		.954 0	1.64	
30	63.568 520 (10)		17		.689 8	1.59	
	64.127 777 (20)		19		.465 6	1.54	
	64.678 92		21		.294 2	1.50	
	65.224 120 (20)		23		.174 4	1.45	
	65.764 744 (20)		25		.097 07	1.41	
35	66.302 06		27		.050 82	1.41	
	66.836 77		29		.025 04	1.41	
	67.369 51		31		.011 62	1.41	
	67.900 73		33		.005 08	1.41	
	68.430 8		35		.002 10	1.41	
40	68.960 1		37		.000 815	1.41	
	69.488 7		39		.000 299	1.41	
	70.016 9		41		.000 104	1.41	
	70.544 9		43		.000 034	1.41	
44	118.750 343 (10)			1	.597 3	1.96	

99% of total 60 GHz O_2-MS intensity
T = 200° K
T = 300° K

Note: ( ) Measured value; digits in parenthesis represent the standard deviation of that value in terms of the final listed digits.
*) Center frequencies for $N^{\pm} = 45$ to 63 are given in [2].

C. *The Linewidth Parameter of the O_2–MS*

While the theory of spectral properties (center frequency ν_0 and strength S) relating to the O_2 molecule is well understood, this is not the case for the intensity distribution, especially when considering the full range of meteorological conditions. The atmospheric O_2–MS needs to be discussed separately for two pressure ranges: I—*Isolated Line Spectrum* for $p < 10$ torr ($h > 25$ km); II—*Continuum Spectrum* for $p > 300$ torr ($h < 10$ km), where the envelope is determined by all lines.

In *range I*, the pressure-broadened linewidth is

$$\gamma = \gamma^0[m(300/T)^u p + m_w(300/T)p_w]. \quad (8)$$

The width parameter γ^0 belongs to a self-pressure-broadened O_2–MS line and m, m_w are dimensionless broadening efficiencies for dry air and water vapor, all at 300 K; u is a temperature exponent. Theory predicts a quantum

number N-dependence of γ^0 [3], [17]. The width parameters listed in Table I are scaled down by a factor 0.942 from results reported in [16] in order to match experimental 9^+ and 7^+ values (see Table I). The N-dependence is then approximated by

$$\gamma^0 = 1.98 - 0.023N \text{ MHz/torr} \qquad (8a)$$

for $N < 25$, and is assumed constant for $N \geq 25$.

From laboratory measurements of the 9^+ line these results were deduced as follows (p = 1–100 torr) [2].

1) $S^0\psi(T)$—the deviation from theoretical values [Table I, (7)] is zero at 325 K and increases to -5 percent at 252 K within an experimental error of smaller than ± 2 percent.

2) The line shape is verified as being Lorentzian (3), (4).

3) The broadening parameters are

$$\gamma^0(9^+) = 1.77(2) \text{ MHz/torr}, \quad u = 0.85(2)$$

$$m(9^+) = 0.93(1) \quad \text{and} \quad m_w(9^+) = 1.25(5).$$

Additional experimental results on resolved O_2–MS lines are reported in [2], [10], [18].

Considering the 9^+ line in dry air at 300 K and 1 torr as an example yields the following: $i = 25$, $\nu_0 = 61.151$ GHz, $S^0 = 1.590 \cdot 0.2090$ Hz/torr, $\gamma^0 = 1.77 \cdot 0.93$ MHz/torr. The maximum attenuation occurs for $z = 0$, yielding $\alpha_0 = 0.182 \cdot 61.15 \cdot 1.59 \cdot 0.209/1.77 \cdot 0.93 = 2.25$ dB/km; the peak dispersion occurs for $z = \pm 1$

$$\Delta\phi_0 = \pm 20.95 \cdot 10^{-3}(61.151 \mp 0.00167) \cdot 1.59 \cdot 0.209/1.65$$

$$= \pm 0.258 \text{ rad/km}.$$

Two things happen to an isolated O_2–MS line when the pressure drops below 1 torr ($h > 40$ km).

1) Collision-broadening becomes sufficiently small that it does not mask the Zeeman splitting which spreads the many Zeeman components over a 1–2-MHz-wide band around the center ν_0 when the earth's magnetic field is present. The Zeeman spectrum of a line is treated similarly on a megahertz frequency scale as the O_2–MS on a GHz scale. Anomalous emission data indicate that nonlinear overlap effects may modify the envelope of the Zeeman components [14].

2) Each Zeeman component undergoes a gradual transition from collision to Doppler broadening as described by the Voigt profile [1]. The linewidth assumes a pressure-independent value

$$\gamma_D = 6.34 \cdot 10^{-2}\nu_0(T)^{1/2} \text{ kHz}$$

$$\text{(e.g., } 9^+, \text{ 300 K, } \gamma_D = 67.2 \text{ kHz)} \qquad (9)$$

and the shape changes to a Gaussian intensity distribution. As the pressure becomes very small (< 10 m·torr), the rate for attenuation and phase dispersion to approach zero is proportional to S^0p/γ_D.

In *range II*, the addition of individual line shapes around 60 GHz may not be a valid procedure since the increasing number of collisions alters the molecular energy levels to an extent that they can interfere with each other [3], [17]. As a consequence, the intensity distribution of the continuum spectrum deviates from the linear addition of Lorentzians (3), (4). Such redistribution can be accomplished by modifying the linewidth as shown by Meeks and Lilley [12] when attempting to reconcile oxygen attenuation rates [10] between line (I) and continuum (II) spectra. The 1^- line, of course, does not share in the overlap corrections and (8) is valid up to sea level pressures. Cumulative zenith attenuation data have been fitted to such a semiempirical model [20], [22]. The data, measured by the zenith angle technique using the sun as a source, were described when for each line the following was assumed [20]:

$$\gamma_i(p) \approx \gamma^0(h) \cdot p \cdot (300/T)^{0.85} \text{ MHz}. \qquad (10)$$

The width parameter $\gamma^0(h)$ is 1.79 MHz/torr for $h > 25$ km ($p < 20$ torr), linearly decreasing from 1.79 to 0.84 between $h = 25$ and 8 km, and remaining at 0.84 MHz/torr below $h = 8$ km ($p > 180$ torr). The fit to the data which included airplane measurements between $h = 2.6$ and 12.2 km was ± 8.8 percent (squared deviations). Equation (10) becomes the *"CMR-Model"* that is applied in Section III for analysis of atmospheric transfer characteristics.

More extensive, but otherwise similar data [22] were fitted to another width model consisting of a two-piece linear pressure dependence

$$\gamma_i(p) \approx \gamma_c + (1.88/a)(p - p_i)(300/T) \text{ MHz}. \qquad (11)$$

The first range is given by $\gamma < 52.7$ MHz assuming $\gamma_c = 0$, $a = 1$, and $p_1 = 0$; the second range follows for $\gamma \geq 52.7$ MHz assuming $\gamma_c = 52.7$ MHz, $a = 3$, and $p_1 = 20.7$ torr at $T = 222$ K. Equation (11) becomes the *"R-Model."*

Since the abrupt adjustments to the width by either the CMR- or the R-Model are quite arbitrary, a nonlinear expansion of γ in pressure was tried on the published data

$$\gamma_i(p) \approx m(\gamma^0 p - \eta p^2 \cdots)(300/T)^u \text{ MHz}. \qquad (12)$$

Equation (12) becomes with $m = 0.93$, $\gamma^0 = 1.79$ MHz/torr, $\eta = 0.0016$ MHz/torr^2, and $u = 0.9$ the *"NL-Model,"* reducing γ to $\gamma/3$ at 760 torr.

D. Attenuation and Dispersion Due to Water Vapor

Two rotational lines of H_2O are centered on either side of the 40–140-GHz band. The low-frequency wing of the complete H_2O rotational spectrum and additional polarization mechanisms also contribute to atmospheric transfer characteristics. The resonant part due to the two lines is evaluated by (2) [$N_w'' = \sum_r (SF'')_r$ and $\Delta N_w = \sum_r (SF')_r$] assuming for the strengths [25]

$$S = S^0(300/T)^{3.5} p_w \exp[W(1 - 300/T)] \text{Hz} \qquad (13)$$

and replacing the Lorentzian shape $F_L' = z/\gamma(1 + z^2)$, $F_L'' = 1/\gamma(1 + z^2)$ by the *Gross* shape which gave a better fit to measured water vapor attenuation in the wings of strongly air-broadened H_2O lines

$$F_G' = 2\nu_0(\nu_0^2 - \nu^2)/[(\nu_0^2 - \nu^2)^2 + (2\nu\gamma)^2]$$

$$F_G'' = 4\nu^2\gamma/[(\nu_0^2 - \nu^2)^2 + (2\nu\gamma)^2]. \qquad (14)$$

TABLE II
SPECTROSCOPIC PARAMETERS OF THE TWO H_2O MICROWAVE LINES

Label	r	1	2	
Center Frequency	ν_o	22.23515	183.31012	GHz
Strength Parameter	S^o	13.9(3)	322	Hz/torr
Temperature Exponent	W	2.14	0.653	1
Width (H_2O)	γ^o	18.0(2)	19	MHz/torr
Broadening Eff. (Air)	m_d	0.209(1)	0.21	1

The linewidth is given by

$$\gamma = \gamma^0[m_d(300/T)^{0.6}p + (300/T)p_w]\ \text{MHz}. \quad (15)$$

The line parameters are at $T = 300$ K [25] in Table II.

The contributions of these two H_2O lines are not enough to account for millimeter wave attenuation of water vapor away from the two line centers [23]. Laboratory measurements at 61.2 and 30.6 GHz yielded for pure water vapor anomalous high absorption (<1 dB/km) when the saturation pressure was approached [2].

III. ATMOSPHERIC TRANSFER CHARACTERISTICS DUE TO THE OXYGEN MICROWAVE SPECTRUM

The results of Section II for (1) reflect the physical nature of molecular effects characterizing frequency-selective filter properties inherent to the gaseous atmosphere over the ~40–140-GHz range. It is unavoidable to use judicious approximations to get answers for practical problems. A rule-of-thumb approach involves modeling pressure and temperature profiles for slant paths from different heights and at different elevation angles and making several assumptions as follows.

1) Time-variable effects due to turbulence [15] or refractive layers are not treated.

2) The air is dry ($p_w = 0$).

3) The *Lorentzian* shape is valid between $h = 0$ to 80 km.

4) The linewidth of each O_2-MS line is given by

$$\gamma(h) \approx [\gamma(p)^2 + \gamma_0^2]^{1/2}\ \text{MHz} \quad (16)$$

where the constant width $\gamma_0 \approx \gamma_D + 0.9ZH$ approximates Doppler and Zeeman ($Z = 2.803$ MHz/G) broadening, and for $\gamma(p)$ exists the choice of (8), (10)–(12).

5) The U. S. Standard Atmosphere [7] models $p(h)$ and $T(h)$. The earth atmosphere has only a weak dependence on geographic coordinates and in the first approximation it can be considered as a layered homogeneous medium.

A. Homogeneous Path Models

The structure of the transfer function of a homogeneous path is analyzed by means of (2)–(4), (6), (7), and a suitable choice of the width model. Examples of calculated attenuation and dispersion curves at $h = 0$, 10, and 20 km are shown in Fig. 1. A graphical presentation provides a better overview of the transfer characteristics (computer printouts are available upon request). The O_2-MS at $h = 0$ shows a continuum spectrum. The

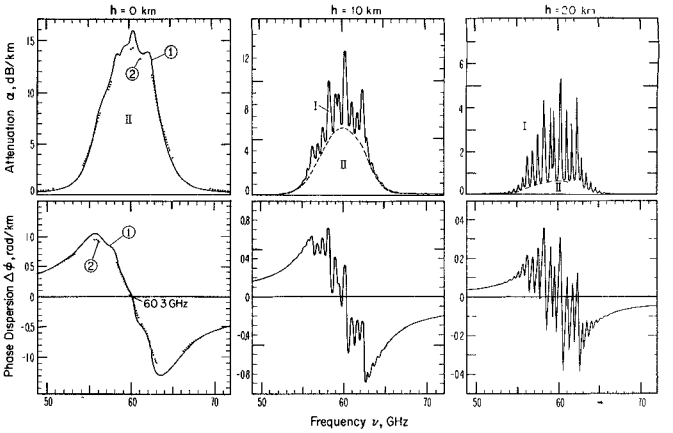

Fig. 1. Horizontal, homogeneous attenuation and phase dispersion rates between 49 and 72 GHz for dry air at the altitudes, $h = 0$, 10, 20 km.

h, km	p, torr	T, K	γ_i, MHz
0	760	288	① 666, ② 968
10	199	233	255
20	41.5	216.5	86.6

envelope is not very sensitive to the individual linewidth, of which two values have been used: 1) $\gamma_i^0 = 0.876$ (CMR-Model) and 2) $\gamma_i^0 = 1.27$ MHz/torr.

The atmosphere acts as a frequency-variable attenuator and the rate of change (≈2.5 dB/km GHz) is nearly constant over ±2-GHz bands centered at 56 and 64 GHz. At $h = 10$ and 20 km the CMR-Model is applied. A mixture of continuum and line spectra exist and the influence of the width becomes more pronounced. At $h \geq 30$ km we have a string of O_2–MS lines.

The sensitivity of these "frozen" transfer characteristics to small variations in pressure or temperature is also of practical interest (e.g., remote sensing of atmospheric conditions, damping of scintillation spectra). Fig. 2 gives an example of sensitivity coefficients a_T (p = const) and a_p (T = const) for oxygen attenuation in dry air; more extensive results (40–140 GHz, 200–300 K, 190–760 torr) are given in [2]. These derivatives were calculated using the Linear Width Model (8), and the results will be different for other models such as (10)–(12).

At $h = 50$ km the 9^+ line is chosen to demonstrate the more detailed [when compared with the scalar equation (16)] influence of the earth's magnetic field. The effects of Zeeman splitting depicted in Fig. 3 are for the case of linearly polarized radiation. Each of the 19π — (H is parallel to the transverse magnetic microwave field component $\mathcal{G}$)[4] or 38σ — ($H \perp \mathcal{G}$)[4] components is treated as an individual line and the contributions are summed up over frequency [1]. In general, each $N^{\pm}$ line (Table I) splits into $3(2N \pm 1)$ components. Individual components are not resolved. The 9^+ line (and so does each O_2–MS line) assumes a constant width under the influence of a magnetic field and at $h = 50$ km the maximum attenuation is reduced by 20–36 percent, respectively, for π- and σ-envelopes. The anisotropic transfer characteristics re-

[4] This is the correct orientation contrary to the one given in [1, p. 16].

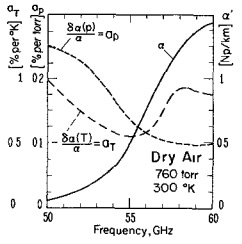

Fig. 2. Pressure and temperature sensitivity coefficients a_p (per torr increase) and a_T (per degree Kelvin decrease) for an example of O_2 continuum spectrum absorption α' (Np/km) between 50 and 60 GHz (1 Np = 8.686 dB).

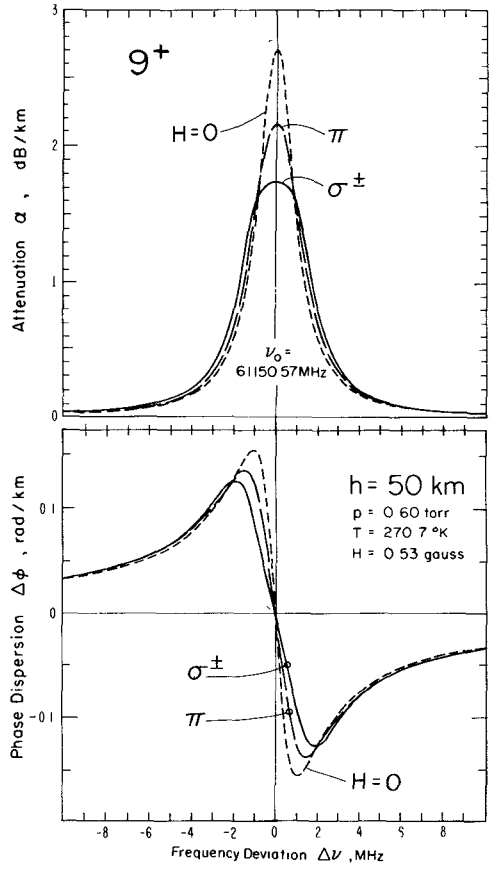

Fig. 3. Effect of Zeeman-splitting upon the homogeneous attenuation and phase dispersion rates at $h = 50$ km in the vicinity ($\Delta\nu = \nu - \nu_0$) of the 9^+ line of the O_2-MS for linearly polarized radiation. The pressure-broadened width is $\gamma(p) = 1.10$ MHz (8).

quire the determination of the type of polarization for the radiation field and the definition of the orientation between H and the magnetic field component $\mathcal{G}$, as it is done in tensor form in [13].

O_2-MS data on phase dispersion are not readily available. The molecular resonance dispersion extends over a larger frequency range. Fig. 4 shows for the examples, $h = 0$ and 10 km, the phase dispersion over the 10–140 GHz range. A differential phase measurement of opposite signs at frequencies in the wing of the O_2-MS offers the potential to follow air and water vapor fluctuations separately in real time as they occur as spatial averages along line-of-sight paths [19]. The gradient of dispersion versus frequency at $h = 0$ km is around 50 and 70 GHz $\sim$

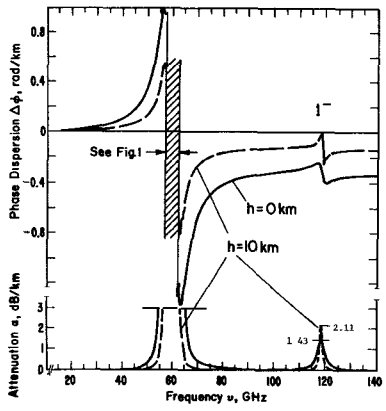

Fig. 4. Phase dispersion and attenuation of dry air in the wings (10–140 GHz) of the O_2 microwave spectrum for homogeneous paths at $h = 0$ and 10 km ("CMR-Model," see Fig. 1).

0.1 rad/km GHz (Fig. 4) and around 60 GHz ~ -0.4 rad/km GHz (Fig. 1), so communication systems may suffer bandwidth limitations [5].

B. Slant Path Models

Cumulative transfer characteristics along a ray trajectory are defined by

$$A = \int_{h_i}^{\infty} \alpha(l)\, dl \quad \text{and} \quad \Delta\Upsilon = \int_{h_i}^{\infty} \Delta\phi(l)\, dl \qquad (17)$$

where dl is the increment of the ray path and h_i is the initial altitude. In general, the integration has to be performed along a trajectory which is curved due to refractive gradients, dN/dh. We assume a straight-line slant path with the increment $dl(\theta) \approx \Delta l(\theta)$ determined by an algorithm based on the starting angle against zenith, θ and a spherically stratified atmosphere which was divided into slabs of thickness Δh [1]. The altitude increments Δh were chosen so that each layer was quasi-homogeneous ($\Delta p < 10$ torr and/or $\Delta T < 2$ K across each slab) amounting to a number of $n = 151$ for $h = 0$ to 80 km. Subsequently, a numerical integration based on Simpson's rule was employed to compute (17)

$$A \approx \sum_n 0.5(\alpha_n + \alpha_{n+1})\Delta l_n(\theta)$$

and

$$\Delta\Upsilon \approx \sum_n 0.5(\Delta\phi_n + \Delta\phi_{n+1})\Delta l_n(\theta). \qquad (18)$$

A computer program was developed for evaluations of (18). The routine was tested for the two extreme cases, zenith ($\theta = 0°$) and tangential ($\theta = 90°$) paths. Examples of calculated attenuation and dispersion curves are shown in Figs. 5 and 6 using the CMR-Model (10) in (16) and $\gamma_0 = 1$ MHz. The zenith path spectra are labeled by the initial altitude h_1; tangential spectra are identified by the height h_0, marking the closest approach to sea level of a tangent through the total atmosphere.

In view of the approximations made for evaluating A and $\Delta\Upsilon$ we hesitate to quote absolute transmission factors.

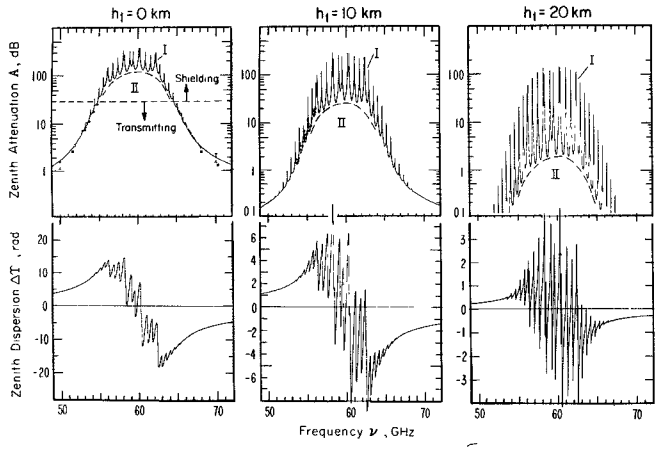

Fig. 5. One-way attenuation A and phase dispersion $\Delta\Upsilon$ due to the O_2–MS between 49 and 72 GHz for a zenith path through the U. S. Std. Atm. 62 [7] from three different initial altitudes h_1 to outer space (I—line, II—continuum spectra). The experimental data at $h_1 = 0$ km (sea level) are listed in Table III and the data at $h_1 = 10$ km are from [20], actually measured at $h_1 = 9.1$ km.

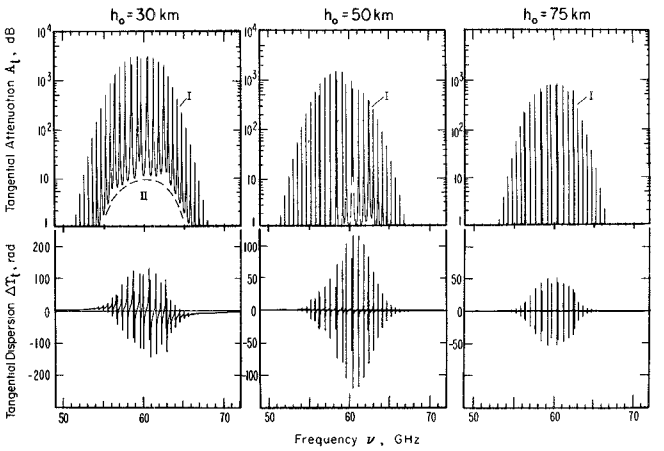

Fig. 6. One-way tangential attenuation A_t and dispersion $\Delta\Upsilon_t$ due to the O_2–MS between 49 and 72 GHz for a straight-line path through the total U. S. Std. Atm. 62 [7] for three different minimum altitudes above ground, $h_0 = 30$, 50, and 75 km (I—line, II—continuum spectra).

TABLE III

ZENITH OXYGEN ATTENUATION A AND EFFECTIVE HEIGHT h_α FROM SEA LEVEL BETWEEN 50 AND 72 GHz

Frequency	MEASURED Reference [No.]	Year	RMS-Uncertainty	Mean Value	CALCULATED Eq: Model: (10) "CMR"		(11) "R"	(12) "NL"	(8) "Linear"
ν			$\pm\delta\bar{A}$	$\bar{A}$	A	h_α	A	A	A
GHz			%	dB	dB	km	dB	dB	dB
50.00	24	1957	15	1.3	(Fig.5)				
	22	1972	7.1	1.12	1.33	5.1	1.09	1.54	2.42
50.20	"	"	9.9	1.31	1.42	5.1	1.16	1.64	2.58
50.70	"	"	6.3	1.58	1.68	5.1	1.38	1.93	3.03
51.25	"	"	12.6	1.98	2.09	5.0	1.73	2.40	3.70
51.75	"	"	11.1	2.43	2.62	5.0	2.18	2.98	4.53
52.22	"	"	4.8	2.92	3.36	5.0	2.83	3.81	5.60
52.50	(1)*	1969	≈20	5.1	4.03	5.1	3.48	4.52	6.47
53.40	20	1968	5.2	7.16	7.42	5.4	6.59	8.25	10.6
	22	1972	3.0	7.06					
53.50	(1)*	1969	≈20	9.3					
	20	1968	6.7	7.82	8.21	5.6	7.45	8.94	11.4
	22	1972	4.0	8.05					
	"	"	2.9	7.84					
53.811	20	1968	5.4	10.20	10.1	5.6	9.07	11.0	13.7
	22	1972	5.9	9.59					
54.352	20	1968	1.4	15.39					
	"	"	2.8	15.62	15.5	6.0	14.2	16.6	19.4
	22	1972	3.9	13.91					
54.895	20	1968	5.6	23.35	23.8	6.5	22.2	25.4	27.8
	22	1972	4.1	20.89					
60.440 Band Center	-	-	-	-	291 (Max)	18.2 (Max)	-	-	-
66.056	22	1972	7.3	8.61	10.7	5.3	9.39	11.8	15.7
66.565	"	"	0.5	6.23	7.78	5.2	6.70	8.68	12.2
67.016	"	"	6.3	4.64	6.09	5.1	5.17	6.84	10.0
67.696	"	"	4.2	3.08	4.44	5.0	3.70	5.04	7.72
68.144	"	"	5.1	2.58	3.75	5.1	3.10	4.27	6.65
68.680	"	"	3.0	2.04	3.15	5.1	2.59	3.60	5.69
69.216	"	"	13.5	1.71	2.72	5.1	2.23	3.12	4.95
69.732	"	"	7.7	1.46	2.40	5.1	1.97	2.76	4.39
70.0	24	1958	16	1.9	2.26	5.1	1.86	2.58	4.15
70.260	22	1972	10.2	1.37	2.14	5.2	1.66	2.45	3.93
72.0	24	1964	25	1.45	1.57	5.2	1.28	1.80	2.88

Note: * Snider and Westwater, cited in [1].

A check at O_2–MS wing frequencies, where experimental A-data are available, shows in Table III that of the four line linewidth models, the "Linear Model" generates the most unreasonable values strongly suggesting overlap effects in the O_2 continuum spectrum. Recent laboratory measurements on oxygen absorption at high pressures (3–400 ktorr) [17] are described by a theory that takes nonlinear overlap into account [3]. Calculations, however, are so involved that for practical purposes only approximations such as (12) appear feasible, maybe with expansions to higher order terms.

C. Discussion

The atmospheric O_2–MS presents a "natural" filter that can be used to advantage in special system applications. The band center (55–65 GHz) is opaque for any source in space affording shielding of satellite-to-satellite (aircraft) links against ground interferences. A measure of the opacity is the ratio $h_\alpha = A/\alpha(h_1)$ which defines the effective height of an atmosphere assumed to be homogeneous (see Table III). A ground-level station receives across the band center molecular emission from the lowest layers raising the noise temperature to the level of the surface temperature [27]. At higher altitudes, the center becomes transparent in 12 channels each capable of several hundred megahertz of bandwidth. The strong frequency dependences of $A(\alpha)$ and $\Delta\Upsilon(\Delta\phi)$ permit frequency diversity and coding techniques such as signal preprocessing by phase-keying. At the O_2–MS band edges the atmosphere is partially transparent so that, for example, Waters was able to detect on the ground the emission of 5 lines (23^-–31^-) originating in the upper stratosphere [14]. Cumulative phase dispersion can be expressed by a differential time delay $\Delta\tau$ of propagating frequency components

$$\Delta\tau = (1/c)\int_L \Delta n\, dl \approx \Delta\Upsilon/2\pi\nu \text{ s.} \qquad (19)$$

While the nondispersive delay due to $N_0(h)$ through the total atmosphere at zenith is about 7 ns, the extreme values due to the O_2–MS dispersion are +0.040 ns at 58.3 GHz and −0.045 ns at 62.6 GHz ($h = 0$ in Fig. 5).

The clean, dry atmosphere sustains a constant mixing ratio up to $h \lesssim 80$ km for all gases which might have a measurable influence upon transfer properties. An exception is ozone with stronger lines at $\nu_0 = 96.2$, 101.7, 110.8, 124.1, 125.4, 136.9, and 142.2 GHz exhibiting maximum zenith attenuations between 0.16 and 0.75 dB [28]. The climatic dependence of O_2–MS zenith attenuation is roughly ±15 percent for arctic and tropical regions, re-

spectively, when compared with the U. S. Standard Atmosphere [21].

IV. CONCLUSIONS

Technically, there are several promising areas that can benefit from O_2–MS transfer characteristics. The translation of molecular theories on millimeter wave properties of air into engineering terms, the description of analytical schemes to predict propagation phenomena on the basis of meteorological variables together with some examples of unique atmospheric transfer properties shall provide a basis for the development of future prospects operating in the 40–140-GHz frequency range.

It is recommended that a manageable theory be brought forward which embraces continuum and line spectra circumventing more or less arbitrary empirical models, and which is supported by reliable data from laboratory measurements.

Note Added in Proof: Such theory has just been presented by Rosenkranz [29].

ACKNOWLEDGMENT

The author wishes to thank W. M. Welch whose development of the computer programs and many helpful discussions were indispensable to this work.

REFERENCES

[1] H. J. Liebe and W. M. Welch, "Molecular attenuation and phase dispersion between 40 and 140 GHz for path models from different altitudes," Office of Telecommunications, U. S. Government Printing Office, Washington, D. C., DoC, OT Rep. 73-10, p. 102, May 1973.

[2] H. J. Liebe, "Studies of oxygen and water vapor microwave spectra under simulated atmospheric conditions," Office of Telecommunications, DoC, OT Rep. 75-00, Mar. 1975 (in review).

[3] a) U. Mingelgrin, "Classical scattering calculations for diatomic molecules and applications to the microwave spectrum of O_2," Office of Telecommunications, U. S. Government Printing Office, Washington, D. C., DoC, OT/ITS Tech. Res. and Eng. Rep. TRER 32, p. 58, July 1972.
b)——, "The microwave dispersion spectrum of O_2," *Mol. Phys.*, vol. 28, pp. 1591–1602, Dec. 1974.

[4] H. J. Liebe, "A pressure-scanning refraction spectrometer for atmospheric gas studies at millimeter wavelengths," Office of Telecommunications, U. S. Government Printing Office, Washington, D. C., DoC, OT Rep. 74-35, p. 118, Apr. 1974.

[5] L. A. Morgan and C. A. Ekdahl, Jr., "MM-wave propagation," Res. and Tech. Div., Rome Air Force Development Center, Griffiss AFB, N. Y., Rep. RADC-TR-66342, p. 123, Aug. 1966.

[6] R. K. Crane, "Propagation phenomena affecting satellite communication systems operating in the centimeter and millimeter wavelength bands," *Proc. IEEE (Special Issue on Satellite Communications)*, vol. 59, pp. 173–188, Feb. 1971.

[7] "U. S. Standard Atmosphere 1962," prepared under the sponsorship of NASA, USAF, and U. S. Weather Bureau, U. S. Government Printing Office, Washington, D. C.

[8] A. C. Newell and R. C. Baird, "Absolute determination of refractive indices of gases at 47.7 GHz," *J. Appl. Phys.*, vol. 36, pp. 3751–3759, Dec. 1965.

[9] J. H. Van Vleck, "The absorption of microwaves by oxygen," *Phys. Rev.*, vol. 71, pp. 413–424, Apr. 1974.

[10] J. O. Artman and H. P. Gordon, "Absorption of microwaves by oxygen in mm wavelength region," *Phys. Rev.*, vol. 96, pp. 1237–1241, Dec. 1954.

[11] S. A. Zhevakin and A. P. Naumov, "Magnetic permeability of molecular oxygen," *Radio Eng. Electron. Phys.* (English transl.), vol. 12, pp. 1249–1252, 1967.

[12] M. L. Meeks and A. E. Lilley, "The microwave spectrum of oxygen in the earth's atmosphere," *J. Geophys. Res.*, vol. 68, pp. 1683–1703, Mar. 1963.

[13] W. B. Lenoir, "Microwave spectrum of molecular oxygen in the mesosphere," *J. Geophys. Res.*, vol. 73, pp. 361–376, Jan. 1968.

[14] J. W. Waters, "Ground-based measurement of mm-wavelength emission by upper stratospheric O_2," *Nature*, vol. 242, pp. 506–508, Apr. 1973.

[15] N. A. Armand *et al.*, "Fluctuation of mm radio waves propagated through a turbulent atmosphere near the oxygen absorption centered at the wavelength of 5 mm," *Radio Eng. Electron. Phys.* (U. S. A.), vol. 18, pp. 492–497, Apr. 1973 (Transl. from Russian).

[16] W. C. Gardiner, Jr., H. M. Pickett, and M. H. Profitt, "Cross sections for reorientation and rotational relaxation of oxygen," *J. Chem. Phys.*, submitted.

[17] U. Mingelgrin, "The pressure broadening of the O_2 microwave spectrum," Ph.D. dissertation, Dep. Chemistry, Harvard Univ., Cambridge, Mass., p. 130, Mar. 1972.

[18] L. G. Stafford and C. W. Tolbert, "Shapes of oxygen absorption lines in the microwave frequency region," *J. Geophys. Res.*, vol. 68, pp. 3431–3435, June 1963.

[19] J. F. Sullivan and H. M. Richardson, "Propagation of 15.3–31.2 GHz and 45–90 GHz coherent signal pairs," in *AGARD Conf. Proc.*, Apr. 1973, pp. 10/1–11.

[20] a) C. J. Carter, R. L. Mitchell, and E. E. Reber, "Oxygen absorption measurements in the lower atmosphere," *J. Geophys. Res.*, vol. 73, pp. 3113–3120, May 1968.
b) "Oxygen absorption in the earth's atmosphere," Aerospace Rep. TR-0200 (4230-46)-3, p. 102, Nov. 1968.

[21] E. E. Reber, R. L. Mitchell, and C. J. Carter, "Attenuation of the 5-mm wavelength band in a variable atmosphere," *IEEE Trans. Antenna Propagat. (Special Issue on Millimeter Wave Antennas and Propagation)*, vol. AP-18, pp. 472–479, July 1970.

[22] E. E. Reber, "Absorption of the 4- to 6-mm wavelength band in the atmosphere," *J. Geophys. Res.*, vol. 77, pp. 3831–3845, July 1972.

[23] R. K. Poon, "Atmospheric opacity near 0.5 cm wavelength," Ph.D. dissertation, Dep. Elec. Eng., Mass. Inst. Technol., Cambridge, Mass., p. 354, May 1974.

[24] W. I. Thompson, III, "Atmospheric transmission handbook," NASA, Washington, D. C., Tech. Rep. DoT-TSC-NASA-71-6, p. 290, Feb. 1971.

[25] H. J. Liebe, "Calculated tropospheric dispersion and absorption due to the 22-GHz waver vapor line," *IEEE Trans. Antenna Propagat.*, vol. AP-17, pp. 621–627, Sept. 1969.

[26] R. A. LeFande, "Attenuation of microwave radiation for paths through the atmosphere," Naval Res. Lab., Washington, D. C., NRL Rep. 6766, p. 28, Nov. 1968.

[27] L. V. Blake, "Radar/radio tropospheric absorption and noise temperature," Naval Res. Lab., Washington, D. C., NRL Rep. 7461, p. 79, Oct. 1972.

[28] J. W. Waters, "Ground-based microwave spectroscopic probing of the stratosphere and mesosphere," Ph.D. dissertation, Dep. Elec. Eng., Mass. Inst. Technol., Cambridge, Mass., p. 237, Dec. 1970.

[29] P. W. Rosenkranz, "Shape of the 5-mm oxygen band in the atmosphere," *IEEE Trans. Antennas Propagat.*, to be published.